

Mixture of bosonic and spin-polarized fermionic atoms in an optical lattice

Lode Pollet,¹ Corinna Kollath,² Ulrich Schollwöck,³ and Matthias Troyer¹

¹*Theoretische Physik, ETH Zürich, CH-8093 Zürich, Switzerland*

²*Université de Genève, 24 Quai Ernest-Ansermet, CH-1211 Genève, Switzerland*

³*Institute of Theoretical Physics C, RWTH Aachen University, D-52056 Aachen, Germany*

(Dated: December 2, 2024)

We investigate the properties of Bose-Fermi mixtures for experimentally relevant parameters in one dimension using numerical methods. We find that the strong attractive interaction between the bosons and fermions leads to the creation of polaronic particles. The effect of the fermions on the bosons is not only to deepen the parabolic trapping potential, but also to reduce the bosonic repulsion. This reduction would theoretically lead to an increase in the bosonic visibility. The opposite was observed however in the experimental ⁸⁷Rb - ⁴⁰K systems, most likely due to a sharp rise in temperature.

PACS numbers: 03.75.Ss, 03.75.Mn, 71.10.Pm, 71.10.Fd

Systems of interacting bosons and fermions occur frequently in nature. Usually, the bosons act as carriers of force between the fermionic particles. In high energy physics, quarks exchange gluons via the strong force, while in solid state physics electrons can interact via light or lattice vibrations. Most prominent examples of such systems are conventional BCS superconductivity (caused by an effective attractive interaction between the fermions induced by the electron-phonon coupling), the Peierls instability (a charge density wave) and the formation of polarons, which are for example in solids electrons dressed by a cloud of phonons. There are only a few condensed matter systems in which the influence of fermions onto bosons has been investigated. One of them are mixtures of bosonic ⁴He and fermionic ³He, in which a shift of the transition temperature between normal and superfluid ⁴He as a function of ³He concentration was observed.

In the field of ultracold gases fermions and bosons are on an equal footing. The choice of different atomic species [1, 2, 3, 4], the use of Feshbach resonances [5, 6, 7] and optical lattice potentials [8, 9] give almost unrestricted access to all parameters of these systems, offering the possibility to study the influence of the species onto each other and to investigate open questions from other areas of physics in a new context. Theoretical approaches [10, 12, 13, 14, 15, 16, 17, 18, 19] have proposed a whole variety of quantum phases present in homogeneous Bose-Fermi mixtures at low temperature, ranging from a charge-density wave, over a fermionic pairing phase, to polaronic properties, and even to phase separation.

In recent experiments two groups independently succeeded in the stabilization of bosonic ⁸⁷Rb and fermionic ⁴⁰K in a three-dimensional optical lattice [8, 9]. They focused on the loss of bosonic phase coherence and on the increase of the bosonic density varying the fermionic concentration. The trapping potential and the finite temperature make the interpretation of the observed quantities however challenging.

In this Letter, we numerically simulate a one-

dimensional system of interacting bosons and fermions with underlying lattice potential. Our results directly give quantitative predictions for future experiments with an ‘atomic wire’ configuration. Our results are also qualitatively applicable to current three-dimensional experiments [8, 9], since the simulations reveal that the most important mechanisms in trapped mixtures are local.

A mixture of bosonic and spin-polarized fermionic atoms in an optical lattice can be described by the Bose-Fermi Hubbard Hamiltonian,

$$H = - \sum_{\langle i,j \rangle}^L \left(J_B \hat{b}_i^\dagger \hat{b}_j + J_F \hat{c}_i^\dagger \hat{c}_j + \text{h.c.} \right) + \sum_i^L \frac{U_{BB}}{2} \hat{n}_{B,i} (\hat{n}_{B,i} - 1) + \sum_i^L U_{BF} \hat{n}_{B,i} \hat{n}_{F,i} + \sum_i^L \epsilon_{B,i} \hat{n}_{B,i} + \sum_i^L \epsilon_{F,i} \hat{n}_{F,i}, \quad (1)$$

where $\hat{c}_i^\dagger (\hat{b}_i^\dagger)$ and $\hat{c}_i (\hat{b}_i)$ are the corresponding creation and annihilation operators for the fermions (bosons), and $\hat{n}_{X,i}$ is the number operator on site i for species X=B,F. The J_X -terms are the hopping, the ϵ_X -terms describe the external trapping potential, and U_{BB} and U_{BF} denote the on-site interaction strength between bosonic atoms and between a fermionic and bosonic atom, respectively. The effective parameters of the Bose-Fermi Hubbard model are deduced from the experimental parameters of Ref. [8, 9] using a tight-binding approximation [12, 20]. Taking the scattering lengths as $a_{BB}/a_0 = 102 \pm 6$ [21] and $a_{BF}/a_0 = -205 \pm 5$ [22], where a_0 is the Bohr radius, we note that $U_{BF}/U_{BB} \approx -2$, a ratio which is almost constant for all optical lattice depths. We took a wavelength $\lambda = 1064\text{nm}$ for the optical lattice potential, and frequencies $\omega_B = 2\pi \cdot 30\text{Hz}$ and $\omega_F = 2\pi \cdot 37\text{Hz}$ for the harmonic confinement. To determine the state of the mixture we use the canonical two-body Bose-Fermi worm algorithm, a numerically exact Quantum Monte Carlo (QMC) method [10], and the density-matrix

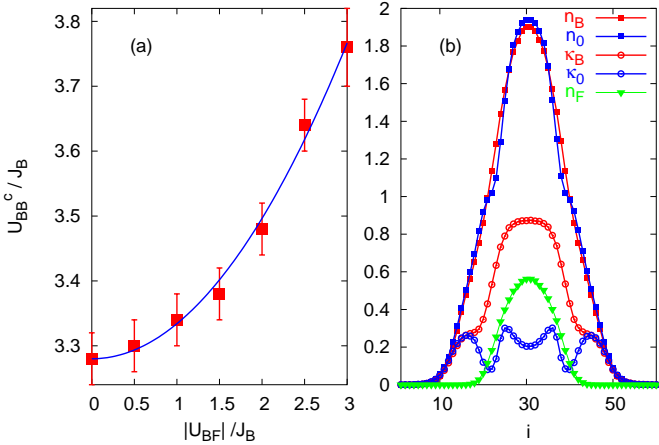


FIG. 1: (Color online) (a) Shift in critical U_{BB}^c for the transition to the Mott phase for attractive U_{BF} . The system consists of 13 fermions, 64 bosons on a homogeneous lattice of 64 sites. Both species have unit hopping and the inverse temperature is $\beta = 64/J_B$. The critical value $U_{BB}^c/J_B = 3.28 \pm 0.04$ at $U_{BF}/J_B = 0$ is taken from Ref. [24]. At finite U_{BF} , the transition is located where the Green function has the same algebraic decay as in the purely bosonic case. The solid curve is a parabolic fit. (b) Comparison between the calculation in the presence of fermions and their approximation by a site-dependent potential for a trapped system of 40 bosons, 8 fermions, inverse temperature $\beta = 1/J_B$ and optical potentials $V_0 = 6E_R$ (or $U_{BB}/J_B = 11.89$). Here, $E_R = \hbar^2 k^2 / 2m_{RB}$ is the bosonic recoil energy. Further, $n_{B(F)}$ denotes the bosonic (fermionic) density for the mixture, n_0 is the density obtained in the approximation. Analogous for the density fluctuations κ_B and κ_0 .

renormalization-group method (DMRG) [11] at zero temperature.

In a mixture, the lowest order effect of the fermions is a shift in the potential experienced by the bosons by $U_{BF}\langle n_{F,i} \rangle$ [12, 23]. In a homogeneous system with a fixed particle number the shift in the potential has no consequences besides adding a constant to the energy. The next order effect is an induced attractive interaction between the bosons [12, 23]. A similar effect is well known from conventional superconductivity, where the phonons (bosons) induce an effective electron-electron interaction. The induced interaction shows up most clearly in a shift of the critical U_{BB}^c/J_B of the bosonic superfluid-Mott transition while varying the interspecies interaction as shown in Fig. 1a). As expected for an induced *attractive* interaction, we find a shift to *larger* values of U_{BB}/J_B . At small U_{BF} the shift is proportional to U_{BF}^2 in agreement with perturbative calculations [23].

In the following we discuss how a parabolic trap and finite temperature change this picture. With a parabolic confining potential the shift in the potential becomes important [12], since this can cause strongly inhomogeneous effective potentials. Note that this mechanism also holds in higher dimensions due to its local character.

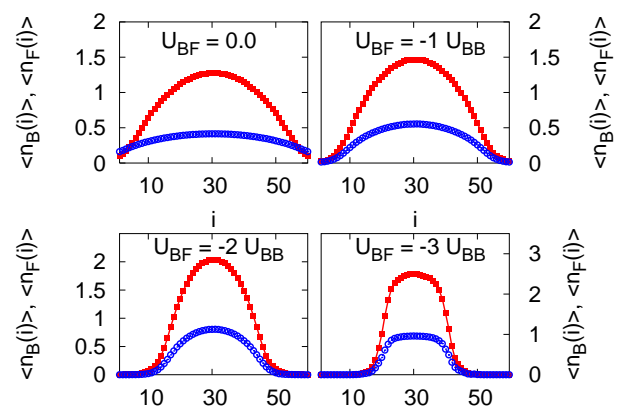


FIG. 2: (Color online) Dependence of bosonic (red, upper curve) and fermionic density (blue, lower curve) profiles on the interspecies interaction strength. In the system there are 50 bosons, 20 fermions, optical potential is $V_0 = 3E_R$ ($U_{BB}/J_B = 4.26$), and the inverse temperature $\beta = 4.26/J_B$.

Fig. 2 shows density profiles for different values of the attractive interaction strength U_{BF} . In the absence of a boson-fermion interaction, all particles are smeared out over the lattice. Turning the interspecies interaction on, we see in Fig. 2 that both species accumulate in the trap center. The fermions are surrounded by a cloud of one to three bosons forming a composite state, which we will call a "weakly-bound polaron". In such a state, the fermions are pinned down in the trap center (cf. Fig. 2), despite their light bare mass. They lower the effective potential in the center of the trap as $U_{BF}\langle n_{F,i} \rangle$, causing the accumulation of bosons.

The effect of an inhomogeneous effective potential can be seen even more clearly by varying the fermionic concentration instead of the interaction strength U_{BF} . In Fig. 3 we show the dependence of the bosonic visibility on the number of fermions with a fixed number of bosons, a setup similar to recent experiments [8, 9]. The bosonic visibility is defined by $\nu = (\rho_B(\pi) - \rho_B(0)) / (\rho_B(\pi) + \rho_B(0))$ where $\rho_B(k)$ is the value of the bosonic momentum distribution at momentum k .

For shallow lattice potentials, a slight increase in the visibility for an intermediate number of fermions is seen. For moderate lattice potentials, on the other hand, one observes a complex, non-monotonic behavior with large variations. If a few fermions are admixed to a bosonic system, the fermions – spreading over several sites in the center of the trap – cause a strongly inhomogeneous effective potential for the bosons. The effective potential exhibits a deep dip in the center of the trap and causes the bosons to accumulate in this region. If the pure bosonic system has a superfluid state (cf. Fig. 3, $N_F = 0$, $V_0 = 3E_R$) the effective potential causes a superfluid state with higher filling in the center of the trap slightly increasing the bosonic visibility. If in the bosonic

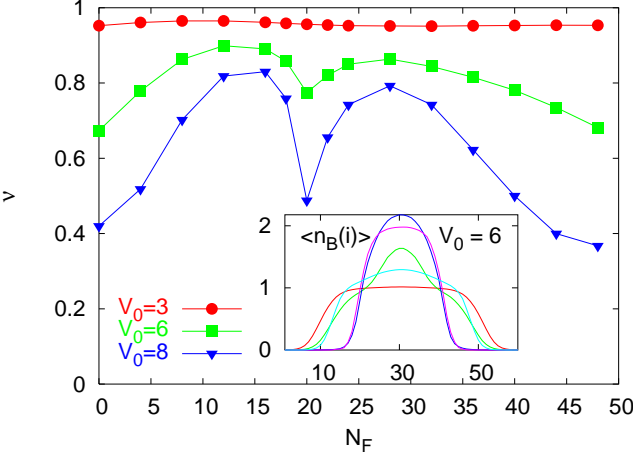


FIG. 3: (Color online) The bosonic visibility ν as a function of fermionic number for a system of $N_B = 40$ bosons and inverse temperature $\beta = 1/J_B$ for different optical potentials $V_0 = 3, 6, 8 E_R$ (or $U_{BB}/J_B = 4.26, 11.89, 21.58$, respectively). The inset shows the bosonic density profiles at $V_0 = 6 E_R$ for $N_F = 0, 40, 4, 20, 16$ bottom to top in the trap center.

system a broad $n_B \approx 1$ plateau (cf. inset Fig. 3, $N_F = 0, V_0 \geq 6 E_R$) was present, it is partly destroyed resulting in a large rise of the visibility. The mechanism holds until there are enough fermions present to form a band insulating region (cf. Fig. 3, $N_F \approx 14$). For such and higher fermion numbers, the effective potential induced by the fermions follows the curvature of the external trap over the region occupied by the fermions with a sudden increase at its boundaries. The number of fermions sets the length of an effective system for the bosons, and controls the bosonic filling. Further increasing the fermion number drives the bosons into a Mott domain [25, 26]. Such insulating regions yield strong dips in the visibility and are formed when $N_F/N_B \approx 0.5$ (also when we take 60 or 20 bosons instead of 40). A further increase in fermion number leads to broad superfluid bosonic regions, causing a high value of the visibility.

In the presence of a confining potential the dominant effect of the fermions on the bosons is thus a modification of the effective trapping potential. This is a local effect and will therefore hold in more general situations such as in higher dimensional systems as realized in recent experiments [8, 9]. However, higher order effects like the induced effective interaction between the bosons influence the actual state of the system and thus cause deviations from the simple picture presented above. In particular, the actual value of the bosonic visibility as shown in Fig. 3 depends on the subtle interplay between all contributing energy scales such as the kinetic energy, the interaction energy, and the potential energy.

To separate the effect of the effective trapping from the induced interaction, we generate an effective site-dependent potential for the bosons by replacing the Bose-Fermi interaction operator by the effective poten-

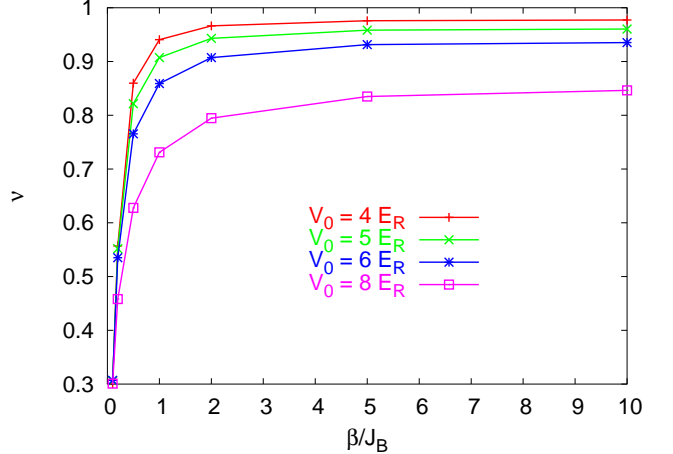


FIG. 4: (Color online) Change in bosonic visibility when inverse temperature β is increased for a system of 50 bosons and 30 fermions.

tial $\mu_i \hat{n}_{B,i} = U_{BF} \langle n_{F,i} \rangle \hat{n}_{B,i}$. This deviates from the disordered chemical potential approach of Ref. [9] and from a mean-field approximation: The exact fermionic density distribution serves as the input for a second, purely bosonic simulation. In Fig. 1(b), we compare the resulting bosonic density and compressibility profiles. We observe that the density profiles are quite well reproduced, confirming that the dominant effect of the fermions is to modify the effective potential for the bosons. However, looking at higher order quantities such as the density fluctuations $\langle n_{B,i}^2 \rangle - \langle n_{B,i} \rangle^2$ we find significant discrepancies. The role of the fermions thus goes beyond the creation of the effective chemical potential for the bosons. In particular, we see Mott plateaus in the approximation that are absent in the full QMC simulation. This is a clear signature for a fermion-induced attractive Bose-Bose interaction, reducing the bare repulsion U_{BB} (cf. Fig. 1(a)). We note, however, that the visibilities are rather well reproduced in the approximation, indicating that the effective potential is the dominant effect as far as the experimental measurements are concerned.

However, in the experiments [8, 9] the presence of fermionic particles induces a *decrease* in the bosonic visibility for moderate values of the lattice potential, in contradiction with the behavior predicted by our results which show an *increase* in the bosonic visibility for most numbers of admixed fermions (in Fig. 3).

The most likely explanation for this discrepancy is a rise in temperature of the mixture when ramping up the lattice [8], as a consequence of the large mass difference. In Fig. 4, we increase temperature (decrease $\beta = 1/k_B T$) at fixed optical potential and atom number. We find a drastic drop in the visibility as temperature is increased for $\beta \approx 2/J_B$. A rise in the temperature of the atoms can therefore cause a decreasing bosonic visibility in the presence of fermions. In fact, a mixture of ^{87}Rb - ^{40}K atoms is likely to become hotter when ramping up the

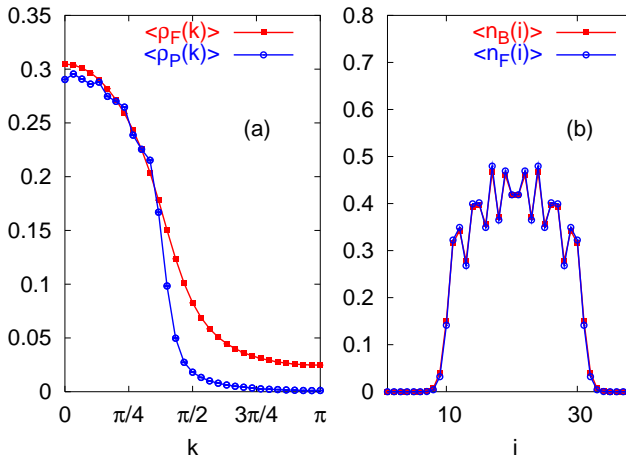


FIG. 5: (Color online) (a) Fermionic $\langle \rho_F(k) \rangle$ and polaronic $\langle \rho_P(k) \rangle$ momentum profiles for the same system. The polarons consist of one boson and one fermion, and the polaronic momentum distribution is given by the Fourier transform of $\langle \hat{b}_i^\dagger \hat{b}_j \hat{c}_i^\dagger \hat{c}_j \rangle$. Error bars are shown, but are smaller than the point size. (b) Bosonic and fermionic ground state density profiles for a system with parameters $N_B = N_F = 8, V_0 = 4E_R (U_BB/J_B = 6.13)$ determined using DMRG (QMC results agree within error bars). The bosonic and fermionic density profiles almost coincide.

lattice [8], making this a very probable explanation of the experimental observation.

We turn now to the regime of low temperatures and low densities. In this regime it turns out that considering the bosons in the mixture as ‘influenced’ by the fermions and not also the other way around is not always a suitable viewpoint. In particular composite pairs of one boson and one fermion *can* be formed for moderately deep optical lattices. First signs of this pairing can be seen

in the polaronic momentum distribution shown in Fig. 5 (a). The momentum distribution of the composite pairs shows a sharper edge than the momentum distribution of the bare fermions. Further the momentum distribution of the composite pairs tends to zero at larger momenta. Thus the composite pairs are better suited to describe the system than the bare bosonic or fermionic particles. Note, that due to the presence of the parabolic confining potential [27] the difference between the pairing and the bare fermionic edge is less pronounced than in a homogeneous system [10]. The description by composite pairs is as well supported by clear coinciding charge modulations in the bosonic and fermionic densities (Fig. 5(b)). For the parameters chosen in Fig. 5(b) the density modulations are mainly due to boundary effects, i.e. Friedel oscillations, but for larger lattice heights the analog of the charge density wave [10, 15] occurs.

In conclusion, we have simulated the trapped one-dimensional Bose-Fermi Hubbard model. The interplay between temperature, trap, optical potential and particle number is very rich and non-universal. The dominant effect is the creation of a strongly inhomogeneous trapping potential by the fermions. In higher order the fermions induce an attractive interaction between the bosons, which should lead to an increase in the bosonic visibility. However assuming a rise in temperature when ramping up the lattice, a decrease in the visibility is found analogous to the experimental observation in the ^{87}Rb - ^{40}K samples.

We are grateful to H. P. Büchler, T. L. Ho, A. Muramatsu, G. Pupillo, B. V. Svistunov and the group of T. Esslinger for stimulating discussions. We acknowledge support by the Swiss National Science Foundation and the Aspen Center for Physics. Simulations were performed on the Hreidar Beowulf cluster at ETH Zurich.

[1] A. G. Truscott *et al.*, *Science* **291**, 2570 (2001).
[2] F. Schreck *et al.*, *Phys. Rev. Lett.* **87**, 080404 (2001).
[3] G. Modugno *et al.*, *Science* **297**, 2240 (2002).
[4] C. Silber *et al.*, *Phys. Rev. Lett.* **95**, 170408 (2005).
[5] S. Ospelkaus *et al.*, *Phys. Rev. Lett.* **97**, 120403 (2006).
[6] Z. Hadzibabic *et al.*, *Phys. Rev. Lett.* **91**, 160401 (2003).
[7] S. Inouye *et al.*, *Phys. Rev. Lett.* **93**, 183201 (2004).
[8] K. Günter *et al.*, *Phys. Rev. Lett.* **96**, 180402 (2006).
[9] S. Ospelkaus *et al.*, *Phys. Rev. Lett.* **96**, 180403 (2006).
[10] L. Pollet *et al.*, *Phys. Rev. Lett.* **96**, 190402 (2006).
[11] S. R. White, *Phys. Rev. Lett.* **69**, 2863 (1992); U. Schollwöck, *Rev. Mod. Phys.* **77**, 259 (2005).
[12] H. P. Büchler and G. Blatter, *Phys. Rev. Lett.* **91**, 130404 (2003).
[13] M. Cazalilla and A.F. Ho, *Phys. Rev. Lett.* **91**, 150403 (2003).
[14] M. Cramer, J. Eisert and F. Illuminati, *Phys. Rev. Lett.* **93**, 190405 (2004).
[15] L. Mathey *et al.*, *Phys. Rev. Lett.* **93**, 120404 (2004).
[16] M. Lewenstein *et al.*, *Phys. Rev. Lett.* **92**, 050401 (2004).
[17] A. B. Kuklov and B. V. Svistunov, *Phys. Rev. Lett.* **90**, 100401 (2003).
[18] A. Albus, F. Illuminati, and J. Eisert, *Phys. Rev. A* **68**, 023606 (2003).
[19] A. Imambekov and E. Demler, *cond-mat/0510801* (unpublished).
[20] D. Jaksch *et al.*, *Phys. Rev. Lett.* **81**, 3108 (1998).
[21] Ch. Buggle *et al.*, *Phys. Rev. Lett.* **93**, 173202 (2004).
[22] F. Ferlaino *et al.*, *Phys. Rev. A* **73**, 040702(R) (2006).
[23] H. P. Büchler and G. Blatter, *Phys. Rev. A* **69**, 063603 (2004).
[24] L. Pollet, PhD-thesis, Universiteit Gent, unpublished. see <http://www.nustruc.ugent.be/thesislode.pdf> (2005).
[25] G. G. Batrouni *et al.*, *Phys. Rev. Lett.* **89**, 117203 (2002).
[26] C. Kollath *et al.*, *Phys. Rev. A* **69**, 031601(R) (2004).
[27] M. Rigol and A. Muramatsu, *Phys. Rev. A* **69**, 053612 (2004).
[28] S. Fölling *et al.*, *Phys. Rev. Lett.* **97**, 060403 (2006).